Modified method of perturbed stationary states. V. Electron-capture cross sections for the reaction $O^{8+}+H(1s)\rightarrow O^{7+}(n,l)+H^{+}$

E. J. Shipsey
Department of Physics, University of Texas at Austin, Austin, Texas 78712

T. A. Green
Sandia National Laboratories, Albuquerque, New Mexico 87185

J. C. Browne
Department of Physics and Department of Computer Science, University of Texas at Austin, Austin, Texas 78712

(Received 28 June 1982)

Electron-capture cross sections are reported for the reaction $O^{8+}+H(1s)\rightarrow O^{7+}(n,l)+H^{+}$, with $n=4,5,6$ and $l=0$ through $n-1$. The cross section for $n=7$ is also estimated. The energy range extends from 13 eV/amu to 34 keV/amu. A Landau-Zener formula is given for use at lower energies. The calculations are quite analogous to those carried out for C^{6+}-H(1s) collisions in Phys. Rev. A 25, 1364 (1982). The modified perturbed-stationary-state calculation features the use of a mixed representation of diabatic and adiabatic states and the use of translation factors determined by Euler-Lagrange optimization within the mixed representation of states. One internuclear separation-dependent factor is used for the initial state, which correlates to $O^{8+}+H(1s)$. A second factor is used for all the $O^{7+}+H^{+}$ correlating states. Riley's semiclassical average approximation is used at low energies and the straight-line impact-parameter method is used at high energies. For the purpose of comparison, some calculations are also carried out by the method of Bates and McCarroll and by that of Piacentini and Salin. The approximation of neglecting π-π and Δ-Δ couplings is tested. The results are compared with those of other researchers.

I. INTRODUCTION

Since the inception of the magnetic fusion energy program a central concern has been the development of diagnostic techniques for the determination of the physical parameters which characterize the time- and space-dependent plasma conditions inside the various experimental devices. This process has gone hand in hand with the development of plasma theory and atomic theory in general, as well as with refinement of the theoretical models of specific experiments.[1]

The primary purpose of the work reported here is to provide charge-exchange cross sections which play a role in models of the x-ray production from radiative decay of excited states of the one-electron ion O^{7+}.[2] One mode of production of these states is through the electron capture reaction, $O^{8+}+H(1s)\rightarrow O^{7+}(nlm)+H^{+}$. In this mode, the states with principal quantum number $n=4$, 5, and 6 have the largest cross sections in the energy range discussed here, namely, H-atom energies up to about 35 keV. This paper provides electron capture cross sections Q_n, $n=4-6$, and for each n, the corresponding atomic angular momentum sublevel occupation probabilities P_l, $l=0$ to $n-1$.

It is difficult to make O^{8+} ions for use in experiments at kilovolt energies and at present no experimental data are available for these particular cross sections. However Afrosimov *et al.* have recently reported results for $O^{8+}-H_2$ collisions.[3] Previous theoretical work on the $O^{8+}-H$ system has provided the total capture cross section for energies in the kilovolt range.[4-9] However, this is the first calculation of the Q_n and P_l for H-atom energies below 25 keV. At higher energies, predictions of the Q_n and P_l are available from Olson's classical-trajectory Monte Carlo work[10] and from the Eikonal calculations of Chan and Eichler.[11]

From the scientific point of view the present work is interesting because it is a nontrivial application of perturbed-stationary-state (pss) theory in an energy range where the formulation of charge-exchange theory itself is a matter of some controversy.[12] In this context the computed cross sections are valuable because of the comparisons which can ultimately be made with measured and other theoretical values.

The details of the theory and of the present

cross-section calculations have been given in earlier papers in this series.[13–16] In Ref. 13 the literature was reviewed and our approach to perturbed-stationary-states (pss) theory was formulated. In summary, our pss work is based on the semiclassical average approximation[17,14] to the full quantum reaction coordinate formulation of Ref. 13. The semiclassical approximation includes a variationally determined plane-wave translation factor for each basis state in the expansion.[14,18–20] These factors, which depend on the internuclear separation, tend toward the Bates-McCarroll[21] values in the separated atom limit and toward the analogous center-of-charge value in the united atom limit.[14] A mixed representation of adiabatic and diabatic states is used.[13–15] The matrix element calculations are carried out in such a way that no power-series expansions in impact velocity are made.[15] This allows calculations to be carried out from a few eV/amu to a preselected upper limit, which in this paper is 34 keV/amu. This work is therefore to be compared not only with the lower-energy work based on impact-velocity power-series expansions but with high-energy, atomic-basis, close-coupling formulations as well.

In Ref. 16, calculations for CH^{6+} using variational,[16] Bates-McCarroll,[21] and Piacentini-Salin[22] translation factors were compared. The analogous calculations for OH^{8+} are reported here. It would be of particular interest to have atomic-basis, close-coupling calculations[9] carried out at energies above 1 keV/amu for comparison with the pss results.

The OH^{8+} and CH^{6+} molecular energy-level systems are very similar, especially if a correspondence is made between the level labeled nlm in CH^{6+} with the level labeled $n+1$, $l+1$, m in OH^{8+}. Thus, charge exchange is dominated in CH^{6+} by a 540-430 avoided crossing near $R\sim 8$ a.u. and at very low energy by a 650-540 avoided crossing near $R=21.6$ a.u. In OH^{8+} the analogs are the 650-540 avoided crossing near $R=8$ a.u. and the 760-640 avoided crossing near $R=16.7$ a.u. This is readily appreciated if the potential curves in Fig. 1 are compared with those in Fig. 1 of Ref. 16. In the case of CH^{6+} we treated the long-range avoided crossing in a separate calculation.[23] This is not necessary in the present case.

The previous calculations for O^{8+}-H collisions most closely related to ours are those of Salop and Olson.[4] These authors employed the method of Piacentini and Salin[22] to calculate the total capture cross section for impact velocities between 1 and 12×10^7 cm/sec. We used their results as the starting point for our calculations.

The similarity between the oxygen and carbon systems allowed us to use the same methods in this

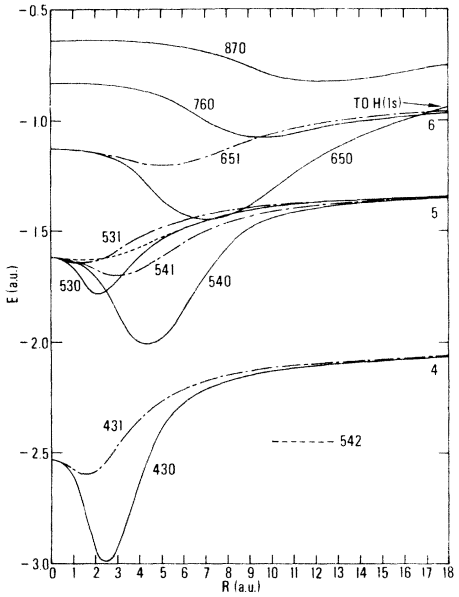

FIG. 1. Electronic energy eigenvalues for OH^{8+}. The curves are labeled by their united-atom quantum numbers nlm. Solid curves represent σ states and dot-dashed curves represent π states. The 542 curve is only shown where it does not overlap the 530 curve. The separated atom states $O^{8+}+H(1s)$ and $O^{7+}(n'l'm')+H^+$ are indicated at the right-hand edge of the curves. Just n' is given for the oxygen-correlating states. The initial channel is $O^{8+}+H(1s)$. The avoided crossing between states 760 and 650 looks like a crossing in the figure. An avoided crossing (not shown) between states 760 and 870 is assumed to be completely diabatic.

paper which were described in Sec. II of Ref. 16. This discussion will therefore not be repeated here. However, there is one new aspect of the oxygen calculations which needs to be discussed. In Ref. 16 it was found (not surprisingly) that to correctly predict the atomic angular momentum sublevel probabilities P_l for a given atomic principal quantum number n, one needed to include all the molecular nlm basis states which correlate to the n manifold in question. The total number of states required for $n=4$, 5, and 6 is 46, to which should be added a few more $n=7$ states for a reasonable calculation. This is more states than our computer program could accommodate without substantial revisions, so we elected to base our results on the approximation described below. In Ref. 16 it was shown by direct tests that the cross section Q_n for a given atomic level n could be obtained to a very good approximation by using the molecular nlm basis states for just the highest two l's (and all m's) which correlate to the n manifold in question. This approximation of using the top two l values is also inherent in a simplified form

in the work of Refs. 4 and 6. The approximation used for the present calculations is to pick one of the three atomic n values of interest, $n=4$, 5, or 6, and use all the molecular nlm basis states for this n. For the other two values of n, the approximation of the top two l's is used. To these states a few $n=7$ states are added. We believe, in qualitative agreement with the model of Abramov, Barishnikov, and Lisitsa,[8] that the atomic sublevel probabilities will be well approximated in this fashion, because for the atomic n level under consideration the nearly degenerate intramanifold couplings are fully taken into account. We do not think that the low-l intermanifold couplings neglected here can alter the computed P_l very much. Thus, in place of one ~ 50-state calculation we have done three 33-state calculations.

As in our previous work a diabatic transform is applied to the avoided crossing near $R=8$ a.u. for the high-energy calculations. In addition, the Landau–Zener-type avoided crossing at $R=16.7$ a.u. is treated by beams of a diabatic transform at all energies.

The large-R avoided crossing can be treated by the Landau-Zener formula at low energy. We find that the corresponding computed cross section agrees well with the Landau-Zener value for an H-atom impact energy of 13 eV.

The scattering bases, translations parameters, diabatic transforms, and types of calculations are described in Sec. II. The results are presented and discussed in Sec. III, in which some general observations are also made.

II. DETAILS OF THE CROSS-SECTION CALCULATIONS

The initial state for the calculation is the united-atom-desgination state 760 which, as indicated in Fig. 1, correlates diabatically to $O^{8+} + H(1s)$. The 760-650 avoided crossing near $R=16.7$ a.u. is always treated diabatically using a two-state transform over the region of internuclear separation R between 15.0 and 18.4 a.u. The transform is obtained as described in the Appendix to Ref. 13. Thus the initial state becomes the state labeled 650 for $R \leq 15.0$ a.u. Following the discussion given in Refs. 15 and 16 we treat the inner avoided crossing between states 650 and 540 in an adiabatic representation for $v \leq 5\times 10^7$ cm/sec and in a diabatic representation for $v \geq 5\times 10^7$ cm/sec. This is done to validate the weak-coupling approximation used in connection with the Euler-Lagrange determination of the translational parameters for the states 650 and 540. Henceforth the words adiabatic and diabatic refer to the representations connected with the transform for the above pair of states. We will say that we are doing adiabatic calculations for $v \leq 5\times 10^7$ cm/sec and diabatic ones for $v \geq 5\times 10^7$ cm/sec even though the outer avoided crossing is always treated diabatically.

The diabatic transform for the 650-540 avoided crossing is defined over the region $R \leq 12.0$ a.u. It is completely analogous to the one used for the 540-430 avoided crossing in CH^{6+} and was determined in the same way. With both transforms in effect, the initial diabatic state is very much like a polarized H(1s) orbital in to $R \sim 7$ a.u., where the inner transform then gradually returns to a nearly diagonal form. Without the inner transform the initial state loses its H(1s) character at larger R.

The inner transform is shown in Fig. 2, which gives the sine of the transform angle as a function of internuclear separation. The translation parameters are also shown in Fig. 2, which should be compared with Fig. 5 of Ref. 15. These parameters appear in the translation factor which multiplies a particular state. The translation factor has the form

$$\exp\{-im/\hbar[U(R)v_z z + G(R)v_x x]\} ,$$

where $U(R)$ and $G(R)$ are the translation parameters in the notation of Refs. 14 and 15, v_x and v_z are

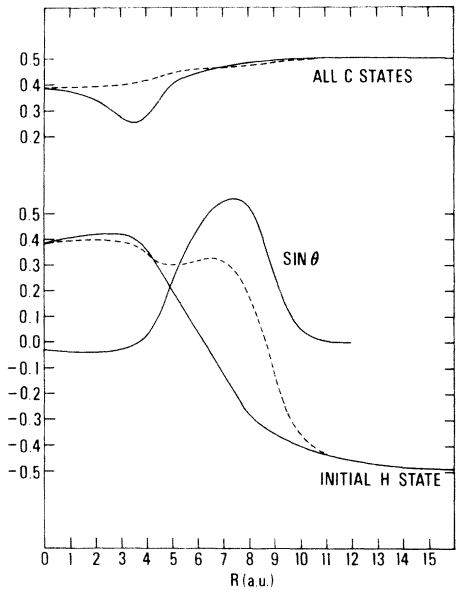

FIG. 2. Translation parameters used in the translation factors for the H(1s) and $C^{7+}(nlm)$ correlating states. The two diabatic parameters are shown as solid curves and the two adiabatic parameters are shown as dashed curves. The curve labeled sinθ is the off-diagonal component of the two-by-two, orthogonal diabatic transform for the avoided crossing between states 650 and 540. States with $n \leq 7$ were included in the Euler-Lagrange formulas [Eqs. (67) of Ref. 14] for the parameters. See Ref. 15 and the text.

the components of the relative velocity, z and x are electron coordinates measured from the midpoint of the internuclear line, and m is the electron mass. The z axis goes from the oxygen to the hydrogen nucleus. Figure 5 of Ref. 15 shows the diabatic $U(R)$ and $G(R)$. The $U(R)$ and $G(R)$ for OH^{8+} are completely analogous. We chose to do this calculation with $\bar{U}(R)=\bar{G}(R)=\frac{1}{2}[U(R)+G(R)]$ because we do not think the difference between $U(R)$ and $G(R)$ is significant given its small size and the approximations made in obtaining the Euler-Lagrange equations of Ref. 14, from which $U(R)$ and $G(R)$ are calculated. Figure 2 shows the two diabatic $\bar{U}(R)$ as solid lines. The two adiabatic $\bar{U}(R)$ are shown as dashed lines.

As stated in the Introduction, we use only two parameters $\bar{U}(R)$; one for the initial state which correlates to H(1s), and a second for all the oxygen-correlating states. The diabatic $\bar{U}$ are the Euler-Lagrange values associated with the diabatic states from the 650-540 transform. Thus the oxygen-correlating parameter is the Euler-Lagrange result for the molecular state 540 for $R \geq 12.0$ a.u. The adiabatic parameter $\bar{U}$ for the initial state is the Euler-Lagrange value for state 650 for $R \leq 15.0$ a.u. The adiabatic oxygen-correlating parameter was chosen to be the Euler-Lagrange value for state 651. This choice, which is not critical, reflects our desire to choose a compromise factor for all the oxygen-correlating states. The variation of Euler-Lagrange $G(R)$ and $U(R)$ from state to state is illustrated by the results for CH^{6+} which are given in Figs. 2–5 of Ref. 15. Figure 8 of this reference shows a test of the effect of the two-parameter approximation on the partial-wave cross section for CH^{6+}. The Euler-Lagrange values of $U(R)$ and $G(R)$ for states 760 and 650 have reached values closely equal to the Bates-McCarroll values ∓ 0.5 by the time R approaches 15.0 a.u., inside the outer crossing. They switch character as the crossing is traversed. Since we treat the outer crossing diabatically, the $\bar{U}(R)$ do not deviate from the Bates-McCarroll values sensibly for $R \geq 15.0$ a.u. For the Bates-McCarroll (BMC) calculations[21] carried out here, the 760-650 avoided crossing was treated diabatically, so as to have the proper factors associated with states 760 and 650 inside the outer crossing. The inner crossing was treated adiabatically. Thus the Bates-McCarroll factors are associated with molecular eigenstates inside $R=15.0$ a.u. The Piacentini and Salin (PS) theory[22] is invariant with respect to diabatic transformations of the type used here.

As mentioned in the Introduction, three calculations were used to find the cross sections Q_n and l-subshell population probabilities P_l for the final nlm states of O^{7+}. The letters A, B, and C have been used to designate the calculations which provide the P_l for $n=6$, 5, and 4, respectively. Since the initial state populates the $n=5$ levels most directly, we consider calculation B, which includes all the $n=5$ correlating states, to be the main calculation. Table I shows the expansion basis for this calculation. The only matrix elements with plane-wave translation factors in their integrands are those for the first 12 states in the first row, and the analogous ones across the diagonal. Because of the two-translation-factor approximation, the other 117 matrix elements are of the usual form. Also the overlap matrix is diagonal, apart from the first row and column. Couplings matrix elements with Δn, Δl, or $\Delta m \geq 2$ are usually omitted. For $\Delta n=0$, couplings for which l and m both change, but in opposite directions, are usually omitted. For $\Delta n=1$ and $\Delta m=0$, couplings for which n and l change in opposite directions are usually omitted. Finally, for $\Delta n=1$ and $\Delta m=\pm 1$, couplings for which l and m change in opposite directions are usually omitted. These approximations were arrived at during the work on the CH^{6+} system by studying the relative sizes of the matrix elements themselves.

Table II describes the other calculations. In addition to the BMC and PS calculations, a B′ calculation was set up to test the accuracy of the commonly used approximation in which π-π, Δ-Δ, etc., couplings are omitted. The Σ-Σ couplings, and those for which $\Delta m \neq 0$, are retained.

On the basis of previous experience on the CH^{6+} system, the straight-line impact-parameter method was used for $v \geq 2\times 10^7$ cm/sec. A simple version of the average approximation[17,14] was used at lower velocities, where no $n=4$ states were included in the expansion bases. In the average approximation only, the initial-state potential curve was used for all states with $n \neq 5$ and that of state 541 was used for all states with $n=5$. The average approximation then uses three potentials for its trajectories: that for the initial state, that for state 541, and the arithmetic mean of the two. At low energy the large-R avoided crossing is adequately treated on the initial-channel trajectory and the near degeneracies of the inner regions are well treated by the arithmetic mean potential and 541 potential. At large impact parameters the inner region is not accessible, and the initial-state potential (including the nuclear repulsion) is nearly zero. For these impact parameters, the straight-line impact-parameter method was used.

The outer crossing causes the partial-wave cross sections to oscillate as a function of system angular momentum L. At high energy about 45 L values were sufficient to obtain the integrated cross sections. At the lowest energy 186 L values were required. For $v \geq 2\times 10^7$ cm/sec the equations were

TABLE I. States of the OH^{8+} molecular ion used in calculation B of Table II. The states are identified in united-atom notation and numbered from 1 to 33. The triangular array shows which couplings between pairs of states were included (F), or omitted (T).

		1	2	3	4	5	6	7	8	9	10	11	12	13	14	15	16	17	18	19	20	21	22	23	24	25	26	27	28	29	30	31	32	33
760	1	F	F	F	F	F	F	F	F	F	F	F	F	T	T	T	T	T	T	T	T	T	T	T	T	T	T	T	T	T	T	T	T	T
650	2		F	F	F	F	F	F	F	F	F	F	F	T	T	T	T	T	T	T	T	T	T	T	T	T	T	T	T	T	T	T	T	T
540	3			F	F	F	F	F	F	F	F	F	F	T	T	T	T	T	T	T	T	T	T	T	T	T	T	T	T	T	T	T	T	T
761	4				F	T	F	T	T	T	T	T	T	T	T	T	T	T	T	T	T	T	T	T	T	T	T	T	T	T	T	T	T	T
651	5					F	F	F	F	T	T	T	F	T	T	T	T	T	T	T	T	T	T	T	T	T	T	T	T	T	T	T	T	T
541	6						T	F	F	F	F	F	F	F	T	T	T	T	T	T	F	F	T	T	T	T	T	T	T	T	T	T	T	T
750	7							F	T	T	T	T	T	T	T	T	T	T	T	T	T	T	T	T	T	T	T	T	T	T	T	T	T	T
640	8								F	F	T	T	T	T	T	T	T	T	T	T	T	T	T	T	T	T	T	T	T	T	T	T	T	T
641	9									F	T	T	F	F	T	T	T	T	T	T	F	F	T	T	T	T	T	T	T	T	T	T	T	T
530	10										F	F	T	T	T	T	T	T	T	T	F	T	T	T	T	T	F	T	T	T	T	T	F	T
430	11											F	T	T	T	T	T	T	T	T	F	T	T	T	T	T	T	T	T	T	T	T	F	T
431	12												T	T	T	T	T	T	T	T	F	F	F	T	T	T	T	T	T	T	T	T	F	F
652	13													F	F	T	T	T	T	T	F	T	T	T	T	T	T	T	T	T	T	T	T	T
642	14														F	F	T	T	T	T	F	F	F	F	T	T	T	T	T	T	T	T	T	T
653	15															F	F	T	T	T	F	T	F	T	T	T	T	T	T	T	T	T	T	T
643	16																F	F	T	T	F	F	F	F	F	T	T	T	T	T	T	T	T	T
654	17																	F	F	T	T	T	F	T	F	T	T	T	T	T	T	T	T	T
644	18																		F	T	T	T	F	F	F	T	T	T	T	T	T	T	T	T
655	19																			T	T	T	T	T	F	T	T	T	T	T	T	T	T	T
531	20																				F	F	T	T	T	F	T	T	F	T	T	F	F	
542	21																					F	F	T	T	T	T	T	T	T	T	T	T	T
532	22																						F	F	T	T	T	T	F	T	F	T	F	
543	23																							F	F	T	T	T	T	T	T	T	T	T
533	24																								F	T	T	T	T	T	F	T	T	
544	25																									T	T	T	T	T	T	T	T	
520	26																										F	T	F	T	T	F	F	
510	27																											F	F	F	T	T	T	
500	28																												T	F	T	T	T	
521	29																													F	F	F	F	
511	30																														F	T	T	
522	31																															T	F	
420	32																																F	
421	33																																	

integrated out to 220 a.u. At the lower velocities, where the outer avoided crossing is very significant, the equations were integrated out to 330 a.u. Exact numerically computed matrix elements were used for $R \leq 20$ a.u.[15,16] Extrapolated values were used for $R \geq 20$ a.u.[16]

We believe that the overall numerical precision of the results is better than 1%.

III. RESULTS AND DISCUSSION

The main results are contained in Tables III and IV. In Table III the results for $n=6$ and 7 come from calculation A, those for $n=5$ from calculation B, and those for $n=4$ from calculation C. Since there are three calculations, there are three values for several of the cross sections Q_n, as shown in Table IV. The extent to which the three values agree is a measure of the accuracy of the approximations of using just the top two l's for a given n in place of all the l's which correlate to that n. In calculations B and C the $n=6$ and $n=7$ probabilities were summed together so that only Q_6+Q_7 is available. No $n=4$ states are included in calculation A and so there is no corresponding value for Q_4 in Table IV. These states were also left out of calculation B for $v=1\times10^7$ cm/sec because the $n=4$ cross sections had already become very small.

A little study of Table IV shows that Q_{tot} is the same for all three calculations to within a few percent. The other cross-section variations are somewhat larger. For these one has to decide what to use for a final answer. We recommend that values from calculation B be used for Q_4, Q_5, Q_{tot}, and Q_6+Q_7.

TABLE II. Brief description of the various calculations for which results are presented in Tables III–V and Fig. 3.

Calculation	Description[a,b,c]
A	All $n=6$ states; no $n=4$; top $2l$'s for $n=5$ except 544; 760, 750, 761, 870.
B	All $n=5$ states; top $2l$'s for $n=6$; 431, 430, 421, 420; 760, 750, 761. See Table I. For the calculation at $v=1\times10^7$ cm/sec, the $n=4$ and $n=7$ states were omitted.
C	All $n=4$ states; top $2l$'s for $n=5$ and $n=6$; 760, 750, 761.
B′	Same as B but with all $\Delta m=0$ couplings omitted except those for $m=0$.
BMC	Calculation B with Bates-McCarroll translation factors. Only the 760-650 avoided crossing treated diabatically.
PS	Calculation B by the method of Piacentini and Salin.

[a]The large-R avoided crossing between states 760 and 650 is always treated diabatically.
[b]Except for BMC and PS, the avoided crossing between states 650 and 540 is treated diabatically for velocities greater than or equal to 5×10^7 cm/sec; it is treated adiabatically at lower velocities. The corresponding translation parameters for calculations A, B, C, and B′ are shown in Fig. 2.
[c]The straight-line impact-parameter method is used for velocities greater than or equal to 2×10^7 cm/sec. The average approximation is used for lower velocities.

To get Q_6 and Q_7 separately, use the value for Q_6+Q_7 from calculation B and the ratio of Q_6 to Q_7 from calculation A as given in Table III. The cross-section values given in Table III should not be used (except for $n=5$) because they come from the three different calculations and, as is readily verified, add up to more than the Q_{tot} from any one of the calculations.

We believe that the calculations are converged to the extent indicated by the variations in Table IV, except for the addition of more states primarily with $n=7$ and $n=8$. Based on our experience with CH^{6+} in going from a modest $n=5$ basis to a complete $n=5$ basis,[16] it is plausible to suppose that a larger basis with states $n\geq7$ could increase the total cross section by an amount equal to Q_7 in Table III.

Table V contains the results of two auxiliary calculations. The entries for $v=5\times10^7$ cm/sec are the results of calculation B done using the adiabatic treatment of the 650-540 avoided crossing. (See footnote b of Table II.) These values are to be compared with the (diabatic) values for the same calculation-B quantities for $v=5\times10^7$ given in Tables III and IV. The point which is verified in Table V is that, at this transition velocity, the diabatic and adiabatic formulations yield cross sections and l-sublevel probabilities which agree to within a few percent. A similar result was obtained for CH^{6+}. The Table V entries for $v=25.5\times10^7$ cm/sec are the results of calculations B done as described in Tables I and II, except that the diabatic oxygen translation parameter of Fig. 2 was replaced by the adiabatic oxygen translation parameter. These entries are to be compared with the calculation-B entries for $v=25.5\times10^7$ cm/sec in Tables III and IV. What is being tested here is the sensitivity of the cross sections to the use of a compromise oxygen translation parameter. It can be seen that changes of a few percent occur in the cross sections, while changes of the order of 15 percent occur in the l-sublevel probabilities.

Table VI presents an alternative calculation of the sublevel probabilities for $n=4$ and 5 in which all molecular states correlating to these two atomic manifolds are included. The other states in the basis were 760, 650, 651, 640, 641, 652, 642, and 653. The $n=7$ and some $n=6$ states in calculation B were replaced by $n=4$ states. This calculation is

TABLE III. Computed n-manifold cross sections Q_n and relative l-sublevel probabilities P_l for capture into states nlm of O^{7+}. Do not add up the Q_n values in this table. See the text and use the Q_{tot} values from Table IV.

Velocity[a]	n[b]	Q_n[c]	P_0[d]	P_1	P_2	P_3	P_4	P_5
0.5	6	12.28	0.114	0.281	0.304	0.204	0.082	0.015
	5	0.806						
1.0	7	0.027						
	6	7.52	0.050	0.142	0.230	0.281	0.217	0.080
	5	5.42	0.103	0.276	0.259	0.191	0.171	
2.0	7	0.098						
	6	14.30	0.076	0.140	0.172	0.178	0.235	0.200
	5	21.82	0.053	0.120	0.183	0.155	0.489	
	4	0.00						
5.0	7	0.185						
	6	14.98	0.054	0.138	0.197	0.218	0.218	0.175
	5	47.24	0.031	0.120	0.278	0.305	0.266	
	4	0.264	0.181	0.352	0.331	0.136		
10.0	7	0.39						
	6	17.78	0.012	0.047	0.072	0.156	0.288	0.425
	5	45.00	0.029	0.097	0.210	0.367	0.297	
	4	3.78	0.144	0.332	0.346	0.178		
15.0	7	1.34						
	6	20.20	0.009	0.022	0.069	0.157	0.269	0.474
	5	36.12	0.023	0.070	0.159	0.304	0.444	
	4	5.31	0.083	0.229	0.358	0.330		
18.0	7	2.23						
	6	20.30	0.011	0.024	0.083	0.162	0.297	0.423
	5	31.55	0.020	0.071	0.140	0.292	0.477	
	4	4.80	0.062	0.185	0.307	0.446		
25.5	7	2.66						
	6	22.86	0.011	0.049	0.059	0.162	0.299	0.420
	5	21.54	0.019	0.062	0.124	0.297	0.498	
	4	2.88	0.029	0.094	0.202	0.675		

[a]Impact velocity in units of 10^7 cm/sec.
[b]Principal quantum number of $O^{7+}(nlm)$.
[c]Cross sections in units of 10^{-16} cm^2.
[d]l-sublevel population probability sums to unity.

similar to one used for CH^{6+}.[16] It should test the influence on the P_l for $n=4$ of having a more complete interaction between the $n=4$ and $n=5$ manifolds. In this sense the P_l for $n=4$ from Table VI should be more reliable than those from Table III. The P_l for $n=5$ are also presented for their informational value. However their reliability is undermined by the omission of states 643, 654, 644, and 655, which ought to be part of the top two l's approximation for $n=6$. The reader will verify that for $v=25.5\times10^7$ cm/sec the Table VI value of P_2 for $n=4$ disagrees with the Table III value by about 25 percent. The other discrepancies for $n=4$ are less than 15%. At the lower velocity, $v=10\times10^7$ cm/sec, the discrepancies in the P_l between Tables III and VI are less than 7%. The reader will also notice that increasing the $n=4$ manifold basis at the expense of the $n=6$ and 7 basis increases the values of Q_4 and decreases that of Q_6+Q_7 and Q_{tot}. No great surprise here. From this exercise we conclude that if very accurate values of the P_l are required for a given n at high energies, it is necessary to include all the molecular states in the manifold for each adjacent value of n for which Q_n is relatively large.

Table IV also presents the results of some additional calculations which are primarily of scientific interest. In the two B′ calculations the $\pi-\pi$, $\Delta-\Delta$, and higher $\Delta m=0$ couplings were eliminated from calculation B. The B′ approximation appears to be fairly good, although the quality of the $n=4$ cross section is degraded.

(BMC) theory cross sections in Table IV are consistent with a trend observed for CH^{6+} in Refs. 15 and 16. In this calculation the inner crossing is

TABLE IV. Comparison of the capture cross sections Q_n resulting from the calculations described in Table II.

Velocity[a]	H laboratory energy[b]	Calculation[c]	Q_4[d]	Q_5	Q_6+Q_7	Q_{tot}[e]
0.5	13.06	A		0.81	12.28	13.09
1.0	52.23	A		5.48	7.55	13.03
		B		5.42	7.55	12.97
2.0	0.209	A		21.93	14.39	36.32
		B	0.00	21.82	14.33	36.15
5.0	1.306	A		47.23	15.17	62.40
		B	0.23	47.24	14.90	62.37
		C	0.26	47.52	14.90	62.68
10.0	5.22	A		46.33	18.17	64.50
		B	4.04	45.00	17.41	66.45
		C	3.78	45.02	17.16	65.96
		B′	5.18	44.56	16.18	64.92
		BMC	3.37	44.72	20.32	68.41
		PS				61.28
15.0	11.75	A		40.03	21.54	61.57
		B	4.97	36.12	21.04	62.13
		C	5.31	35.57	21.64	62.52
		BMC	2.87	44.26	20.84	67.97
		PS				59.63
18.0	17.01	A		34.84	22.53	57.37
		B	4.71	31.55	21.45	57.71
		C	4.80	31.39	21.34	57.53
		BMC	2.80	41.36	21.09	65.26
		PS				56.74
25.5	34.02	A		21.09	25.52	46.61
		B	2.69	21.54	22.36	46.59
		C	2.88	22.24	21.42	46.54
		B′	1.97	20.09	24.07	46.13
		BMC	2.13	27.78	22.26	52.17
		PS				47.73

[a]In units of 10^7 cm/sec.
[b]In units of keV for velocities above 2×10^7; in units of eV otherwise.
[c]See Table II.
[d]In units of 10^{-16} cm^2.
[e]The total capture cross section.

TABLE V. Auxiliary calculations to test the agreement of adiabatic and diabatic formulations and to test the sensitivity of the results to the use of a compromise carbon translation parameter. See the text.

Velocity[a]	P_0[b] Q_4[c]	P_1 Q_5	P_2 Q_6+Q_7	P_3 Q_{tot}	P_4
5	0.032	0.120	0.281	0.306	0.261
	0.23	46.69	14.87	61.79	
25.5	0.022	0.063	0.141	0.277	0.497
	2.81	22.09	22.01	46.91	

[a]Impact velocity in units of 10^7 cm/sec.
[b]l-sublevel probability. Compare with $n=5$ values in Table III.
[c]Cross sections in units of 10^{-16} cm^2. Compare with calculation B values in Table IV.

treated adiabatically. At the higher energies the $n=5$ and total cross sections are found to be larger than those of the diabatic calculations A, B, and C. In Refs. 15 and 16 the difference in results obtained with adiabatic and diabatic formulations was explored in some detail, and it was found that the diabatic transform, more than the translation factors, was responsible. We believe this to be the case here too. Finally, the PS values for Q_{tot}, which are representation independent, agree very well with those from calculation B.

Figure 3 compares total-cross-section values from different sources. This figure was adapted from Fig. 10 of Ref. 4. In Fig. 3 the last three open squares have been replotted to correct a plotting error in the original Fig. 10. Our values of Q_{tot} have been added

TABLE VI. An alternative calculation of the sublevel probabilities for $n=4$ and 5. All molecular states correlating to these two atomic manifolds are included. See the text.

Velocity[a]	P_0[b] P_0[c] Q_4[d]	P_1 P_1 Q_5	P_2 P_2 Q_6+Q_7	P_3 P_3 Q_{tot}	P_4
25.5	0.018	0.055	0.125	0.288	0.514
	0.025	0.102	0.259	0.614	
	2.99	22.71	19.29	44.99	
18.0	0.019	0.057	0.157	0.282	0.485
	0.071	0.199	0.318	0.412	
	4.93	31.81	19.44	56.18	
10.0	0.030	0.098	0.206	0.373	0.293
	0.140	0.328	0.341	0.191	
	3.69	45.67	16.10	65.46	

[a]Impact velocity in units of 10^7 cm/sec.
[b]Sublevel probability for $n=5$. Compare with values in Table III.
[c]Sublevel probability for $n=4$. Compare with values in Table III.
[d]Cross sections in units of 10^{-16} cm^2. Compare with the results in Table IV.

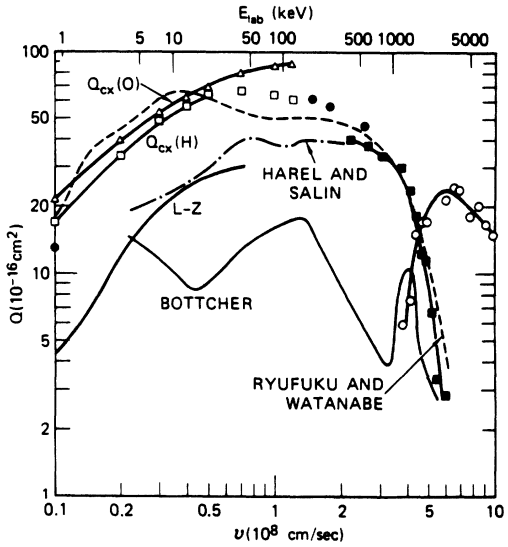

FIG. 3. The total electron capture cross section for $O^{8+}-H(1s)$ collisions. Adapted from Fig. 10 of Ref. 4. The only points added from the present work are those shown as solid circles. Our values for $0.1<v<1.2\times10^8$ cm/sec, as given in Table IV, are not shown because they closely overlap the open squares. From Ref. 4: eight-state pss charge-exchange cross-section values $Q_{cx}(H)$ determined with electron origin on proton, □, and $Q_{cx}(0)$ determined with origin on O^{8+}, △; Monte Carlo charge-exchange values, ■; Monte Carlo ionization values, ○. The lines drawn in for each set of points are intended to guide the eye. The last three open squares, without any guiding line, have been replotted to correct a plotting error in Fig. 10. The Landau-Zener cross section is from Ref. 4. The theoretical cross sections of Bottcher (Ref. 7), Harel and Salin (Ref. 6), and Ryufuku and Watanabe (Ref. 5) are also shown.

as solid circles for $v=10^7$ cm/sec and $v\geq15\times10^7$ cm/sec. The other values fall close enough to the open squares that adding them would have confused the graph. There is a real discrepancy between our results and those of Salop and Olson only for $v=1\times10^7$ cm/sec. We believe this arises from our use of a larger number of partial waves in the determination of the integrated cross sections. The rapid oscillations in the capture probability are shown in Fig. 5 for this velocity. The 3-state PS cross section of Harel and Salin,[6] the 8-state PS cross section of Salop and Olson, and our 33-state PS cross section show how rapidly the PS approach converges for this system, and that it gives very good quantitative results for the total capture cross section.

Our high-energy total cross section is heading toward Salop and Olson's high-energy classical-trajectory Monte Carlo results with a reasonable slope, as was also the case for CH^{6+}.

The total capture cross section agrees well with the unitarized distorted-wave results of Ryufuku and Watanabe.[5] We would hope for such good agreement with distorted-wave, atomic-basis theory at our highest energies and, even at lower energies, we would hope for good agreement of the total capture probability at large impact parameters. This latter point is explored in Figs. 4 and 5. In Fig. 4 the capture probability from calculation B is plotted versus collision angular momentum L for $v=1.5\times10^8$ cm/sec. This velocity corresponds to 11.66 keV/amu. The result obtained by Ryufuku and Watanabe at 10 keV/amu is also shown. The lower unitarized values obtained by them for

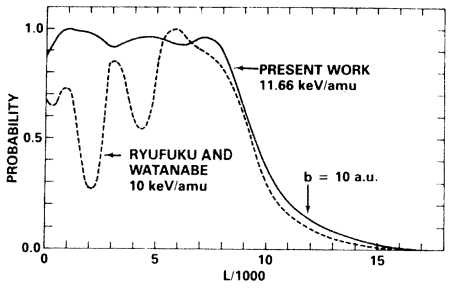

FIG. 4. Plot of medium-energy total electron capture probability versus collision angular momentum quantum number L. The vertical arrow shows the angular momentum corresponding to an impact parameter b equal to 10 a.u. See the text.

$L < 6000$ come from distorted-wave probabilities greater than $(\pi/2)^2$. Our close-coupling calculation leads to probabilities of the order of 0.95. Clearly, the direct use of a weak-coupling approximation is inadvisable for either the atomic or the molecular basis. The large impact-parameter result of the two calculations are in good agreement, however, as regards the effective size of the target for charge exchange.

Figure 5 presents the probability plot for $v=1\times10^7$ cm/sec. This plot should be compared with Fig. 6 of Ref. 5, which corresponds to 50 eV/amu, and which is not reproduced here. Our Fig. 5 shows the oscillations arising from the large-R avoided crossing, which is the primary charge-exchange mechanism for impact parameters b greater than 9 a.u. At smaller impact parameters, these oscillations are superimposed on the much slower oscillations from the inner avoided-crossing region. The reader can verify that there is no physical correspondence at all between our presumably reliable pss result in Fig. 5 and the curve in Fig. 6 of

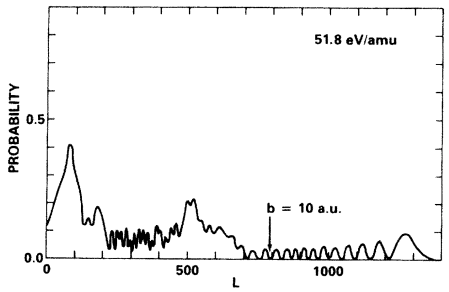

FIG. 5. Plot of the total electron capture probability versus collision angular momentum quantum number L for an impact velocity $v=1\times10^7$ cm/sec. This plot can be compared with Fig. 6 of Ref. 5. The vertical arrow shows the angular momentum corresponding to an impact parameter b equal to 10 a.u. See the text.

Ref. 5. In particular, this latter curve shows a zero probability for impact parameters b greater than 10 a.u., and narrow regions with unitarized probabilities near unity for $b \leq 10$ a.u. These arise when the distorted-wave probability is nearly equal to $(n\pi/2)^2$ for some odd integer n. Nonetheless, on the basis of the total cross section shown in Fig. 3, one might conclude that the theories are in rather good agreement. In the case of CH^{6+} the situation is less confusing, because the total cross sections differ by almost an order of magnitude for $v=1\times10^7$ cm/sec.

There is one final (old) point worth emphasizing about the use of weak-coupling approximations with an atomic-basis expansion at low energy. As Bates and Lynn showed,[24] a two-center atomic-basis close-coupling calculation is equivalent in impact-parameter theory to a molecular calculation carried out with a molecular basis derived from the initial atomic basis. In the case of OH^{8+}, such an approach could deal rather accurately with the large-R avoided crossing whose effects are shown in Fig. 5, and perhaps be acceptable for the inner region as well. An 11-state atomic-basis close-coupling calculation for CH^{6+}, for energies from 0.1 to 1.0 keV/amu, has recently been reported by Fritsch.[9] It is shown that the capture cross section is rather sensitive to the choice of classical trajectory. The use of a bare Coulomb trajectory yields a total capture cross section in close agreement with that of Ref. 16. It is interesting that, in the same energy range, trajectory effects are not very important in the molecular-basis formulation.[25] This state of affairs deserves further study.

The results of Abramov, Baryshnikov, and Lisitsa[8] are not shown in Fig. 3. They lie somewhat above our results at low energy and somewhat below our results at high energy. Their model includes coupling into the atomic manifolds for $n=4$ and 5. These authors have also applied their model to the calculation of the P_l for $n=3$, 4, and 5.[26] Their high-energy results are compared with ours for CH^{6+} in Ref. 16. The comparison would be very similar for OH^{8+}.

The results shown in Fig. 3 due to Harel and Salin, Ryufuku and Watanabe, and Bottcher are discussed in Ref. 4.

As in the case of CH^{6+} it was arranged with Olson to compare our results with his classical-trajectory Monte Carlo results at our highest impact velocity. Some of Olson's unpublished results for OH^{8+} are summarized in Table VII. This energy is below that for which Olson expects the classical-trajectory Monte Carlo method to work best. The results are presented here because of their scientific interest and because our calculation for $v\sim1.2$ a.u. may be pushing the limits of pss theory. The gen-

TABLE VII. Olson's classical-trajectory Monte Carlo cross sections Q_n and l-sublevel population probabilities P_l for an impact velocity of 25.4×10^7 cm/sec. (Private communication based on Ref. 10.)

n[a]	Q_n[b]	P_0	P_1	P_2	P_3	P_4	P_5
≥ 8	2.43						
7	2.55						
6	8.45	0.004	0.037	0.069	0.112	0.229	0.549
5	17.00	0.006	0.040	0.141	0.293	0.520	
4	7.28	0.018	0.143	0.374	0.465		
3	0.35						

[a]Principal quantum number of $O^{7+}(nlm)$.
[b]Cross sections in units of 10^{-16} cm^2.

eral trends of the P_l exhibited in Tables VII and III are in agreement. However some sizable disagreements occur for $n=4$ and 6. This is perhaps not surprising in view of the disagreement about the relative size of Q_4 and Q_6. In the case of CH^{6+} the P_l for $n=3$, 4, and 5 agreed rather well, as is shown in Fig. 3 of Ref. 16. The Q_n values for CH^{6+} were not compared in Ref. 16. In units of 10^{-16} cm^2, our Q_n's were 2.58, 12.29, 20.26, and 1.96 for $n\geq 6$, and $n=5$, 4, and 3, respectively. Olson's corresponding values were 1.48, 3.62, 16.83, and 5.31×10^{-16} cm^2. If we consider the levels 5, 4, and 3 in CH^{6+} to be analogous to the levels 6, 5, and 4 in OH^{8+}, as is suggested by the energy-level diagrams, we see that for both systems the classical-trajectory Monte Carlo method emphasizes transitions to the lower n and deemphasizes transitions to the higher n compared to our modified pss result. We do not have any physical interpretation of this situation at present.

At very low energies, the outer avoided crossing provides the dominant mechanism for charge exchange. In CH^{6+} it was found that the Landau-Zener formula provided a satisfactory estimate of the analogous cross section.[23] For OH^{8+} the Landau-Zener formula yields the result

$$Q_6=\frac{6.179\times10^7}{v(\text{cm/sec})}\times10^{-16}\ \text{cm}^2 \quad (1)$$

for the 760-650 avoided crossing. Equation (1), which is the high-energy version of the Landau-Zener formula,[23] agrees well with Q_6 from Table III for $v=0.5\times10^7$ cm/sec. A study of the post-collision molecular-state occupation probabilities shows, however, that the 650-651 rotational coupling populates the 651 state to a significant degree. (The 652, 640, and 641 states are also populated, but to a minor degree.) Thus the one-state low-energy limit[26] for the P_l is not reached even at this low energy.

ACKNOWLEDGMENTS

The work of A. Salop and R. E. Olson in Ref. 4 was the starting point for the present calculations. We wish to thank R. E. Olson for making unpublished results from his work available to us in the early phases of our project and for carrying out the new calculations presented in Table VII. We wish to thank R. C. Isler, E. C. Crume, and D. F. Post for helpful discussions and information about the role of charge exchange in models of tokamak behavior. We are grateful to T. G. Winter, W. R. Thorson, M. Kimura, J. Vaaben, and D. S. F. Crothers for copies of their manuscripts and information about their work in advance of publication. We wish to thank M. E. Riley for valuable criticism of the first draft of the manuscript. This work was supported in part by the Office of Magnetic Fusion Energy. It was also supported in part by the Office of Naval Research under Contract No. N000-14-67-A-0126-0017 and by the Robert A. Welch Foundation Grant No. F-379.

[1]D. F. Duchs, D. E. Post, and P. H. Rutherford, Nucl. Fusion 17, 565 (1977); A. Nocentini and F. Engelmann, Astrophys. Space Sci. 76, 371 (1981).
[2]R. C. Isler, L. E. Murray, S. Kasai, J. L. Dunlap, S. C. Bates, P. H. Edmonds, E. A. Lazarus, C. H. Ma, and M. Murakami, Phys. Rev. A 24, 2701 (1981).
[3]V. V. Afrosimov, A. A. Basalaev, Yu. S. Gordeev, E. D. Donets, S. Yu. Ovchinnikov, M. N. Panov, and A. N. Zinoviev, in the Book of Abstracts, Proceedings of the XIIth International Conference on the Physics of Electronic and Atomic Collisions, edited by Sheldon Datz (Oak Ridge National Laboratory, Oak Ridge, Tennessee) 1981 (unpublished), p. 692.
[4]A. Salop and R. E. Olson, Phys. Rev. A 19, 1921 (1979).

[5]H. Ryufuku and T. Watanabe, Phys. Rev. A 18, 2005 (1978).
[6]C. Harel and A. Salin, J. Phys. B 10, 3511 (1977).
[7]C. Bottcher, J. Phys. B 10, L213 (1977).
[8]V. A. Abramov, F. F. Baryshnikov, and V. S. Lisitsa, Zh. Eskp. Teor. Fiz. 74, 897 (1978) [Sov. Phys.—JETP 47, 469 (1978)].
[9]W. Fritsch, J. Phys. B 15, L389 (1982).
[10]R. E. Olson, Phys. Rev. A 24, 1726 (1981).
[11]F. T. Chan and Jorg Eichler, Phys. Rev. A 20, 1841 (1979).
[12]J. B. Delos, Rev. Mod. Phys. 53, 287 (1981).
[13]T. A. Green, Phys. Rev. A 23, 519 (1981).
[14]T. A. Green, Phys. Rev. A 23, 532 (1981).
[15]T. A. Green, E. J. Shipsey, and J. C. Browne, Phys. Rev. A 23, 546 (1981).
[16]T. A. Green, E. J. Shipsey, and J. C. Browne, Phys. Rev. A 25, 1364 (1982).
[17]M. E. Riley, Phys. Rev. A 8, 742 (1973).
[18]M. E. Riley and T. A. Green, Phys. Rev. A 4, 619 (1971).
[19]V. H. Ponce, in *Proceedings of the 7th International Conference on the Physics of Electronic and Atomic Collisions,* edited by L. M. Branscomb, H. Ehrhardt, R. Geballe, F. J. de Heer, N. V. Federenko, J. Kistemaker, M. Barat, E. E. Nikitin, and A. C. H. Smith (North-Holland, Amsterdam, 1971), pp. 464—466.
[20]V. H. Ponce, J. Phys. B 12, 3731 (1979).
[21]D. R. Bates and R. McCarroll, Proc. R. Soc. London Ser. A 245, 175 (1958). For an interesting application of this theory to inner-shell excitation, see S. J. Pfeiffer and J. D. Garcia, Phys. Rev. A 23, 2267 (1981).
[22]R. D. Piacentini and A. Salin, J. Phys. B 7, 1666 (1974).
[23]T. A. Green, J. M. Peek, M. E. Riley, E. J. Shipsey, and J. C. Browne, Phys. Rev. A 26, 1278 (1982).
[24]D. R. Bates and N. Lynn, Proc. R. Soc. London, Ser. A 253, 141 (1959).
[25]T. A. Green, M. E. Riley, E. J. Shipsey, and J. C. Browne, Phys. Rev. 26, 3668 (1982).
[26]V. A. Abramov, F. F. Baryshnikov, and V. S. Lisitsa, Pis'ma Zh. Eksp. Teor. Fiz. 27, 494 (1978) [JETP Lett. 27, 464 (1978)].